SAIC-97/1032:APPAT-183

"GLOBAL MAGNETOHYDRODYNAMIC MODELING OF THE SOLAR CORONA"

PROGRESS REPORT: SECOND YEAR

(2/07/96—2/06/97)

SAIC

Science Applications International Corporation

An Employee-Owned Company

NASA CONTRACT: NASW-4968

SPACE PHYSICS SUPPORTING RESEARCH AND TECHNOLOGY (SR&T),

AND SUBORBITAL PROGRAM

PRINCIPAL INVESTIGATOR:

JON A. LINKER

SCIENCE APPLICATIONS INTERNATIONAL CORPORATION

10260 CAMPUS POINT DRIVE

SAN DIEGO, CA 92121-1578

Global Magnetohydrodynamic Modeling of the Solar Corona

P.I.: Jon Linker
Progress Report: Second Year (2/07/96-2/06/97)

Introduction

Here we describe progress performed under Contract NASW-4968, awarded to Science Applications International Corporation, San Diego, for the period 2/07/96 to 2/06/97. Under this contract, we have continued our investigations of the large-scale structure of the solar corona and inner heliosphere using global magnetohydrodynamic (MHD) simulations. These computations have also formed the basis for studies of coronal mass ejections (CMEs) using realistic coronal configurations.

We have developed a technique for computing realistic magnetohydrodynamic (MHD) computations of the solar corona and inner heliosphere. To perform computations that can be compared with specific observations, it is necessary to incorporate solar observations into the boundary conditions (Mikić & Linker 1996; Linker et al. 1996). We have used Wilcox Solar Observatory synoptic maps (collected during a solar rotation by daily measurements of the line-of-sight magnetic field at central meridian) to specify the radial magnetic field (B_r) at the photosphere (in the manner described by Wang & Sheeley 1992). For the initial condition, we use a potential magnetic field consistent with the specified distribution of B_r at the lower boundary, and a wind solution (Parker 1963) consistent with the specified plasma density and temperature at the solar surface. Together this initial condition forms a (non-equilibrium) approximation of the state of the solar corona for the time-dependent MHD computation. The MHD equations are then integrated in time to steady state. Here we describe solutions relevant to a recent solar eclipse, as well as Ulysses observations. We have also developed a model configuration of solar minimum, useful for studying CME initiation and propagation.

1

Progress Summary

(a) Solar Eclipse of October 24, 1995

Solutions obtained in the manner described above can in principle provide a 3D description of the corona and inner heliosphere, including the detailed distribution of magnetic fields, currents, plasma density, and temperature. However, the validity of this approach can only be verified through comparison with observations. As a test of our coronal modeling capability, we used our computations to predict the large-scale structure of the solar corona during the October 24, 1995 eclipse (occuring during Carrington rotation 1901), visible in a number of locations in the eastern hemisphere. We carried out a simulation using photospheric magnetic field data from the previous rotation (Carrington rotation 1900; September 2 – September 29, 1995) on October 5, 1995, and put the results on the World Wide Web (http://www.saic.com/home/solar/prediction.html). We also presented the results at the Sacramento Peak workshop on October 18, 1995 (described by Linker et al. 1996). Figure 1a shows the magnetic field lines from our calculation. The view angle corresponds to the approximate time of the eclipse. The solution shows the formation of helmet streamers; these are regions with closed magnetic fields that trap coronal plasma flowing out of the Sun. Along open magnetic field lines, the solar wind streams freely, reaching supersonic speeds.

To directly compare our results with observations, we develop images of the polarization brightness (pB; proportional to the line-of-sight integral of the product of the electron density and a scattering function that varies along the line of sight). This quantity is frequently observed with coronagraphs. Using the plasma density from our coronal model, we can compute pB to simulate an eclipse or coronagraph image and compare it with the actual data. Radially graded filters are applied to eclipse images to compensate for the rapid fall-off of coronal density with radial distance; we detrend our computed pB in a similar manner. The polarization brightness of the corona predicted by our simulation, as it would be seen on October 24, 1995 at 05:00UT is shown in Figure 1b. Figure 1c shows an image of the eclipse taken by F. Diego of University College, London, and supplied

to us by Serge Koutchmy of Institut d'Astrophysique, Paris, CNRS. The helmet streamers and open field regions predicted by the computation agree reasonably well with the eclipse observations. We have performed a similar comparison for the November 3, 1994 eclipse and Carrington Rotation 1888 (Mikić and Linker 1996; Linker et al. 1996). These computations confirm the long-held belief that the magnetic field distribution on the Sun controls the position and shape of the streamer belt.

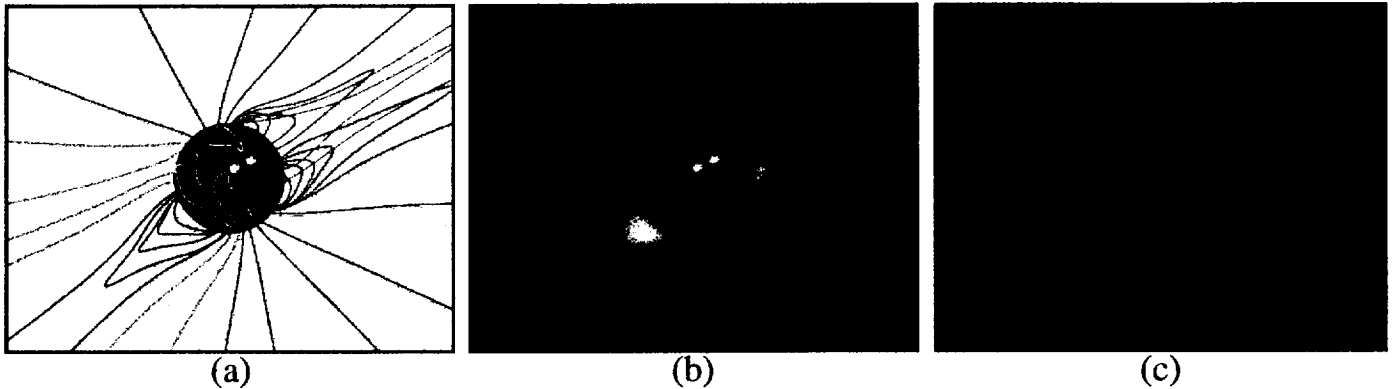(a)   (b)   (c)

Figure 1. A prediction of the structure of the solar corona during the Oct. 24, 1995 solar eclipse. The MHD simulation was carried out on Oct. 5, 1995 using Wilcox synoptic magnetic data for the previous rotation. (a) Field lines and (b) polarization brightness computed from the simulation. (c) Eclipse photograph taken by F. Diego (UCL) in white light with F=910 mm and a two-second exposure time.

(b) Comparisons with Ulysses Data

We have also compared the results of our calculations to interplanetary observations. As a first test, we computed an MHD model of the solar corona for Carrington rotation 1869 (May–June 1993). This rotation was of particular interest for Ulysses observations, as the Ulysses spacecraft ceased to observe sector-boundary crossings during that time period (Smith et al. 1993). Figure 2 shows a comparison of the heliospheric current sheet (HCS) predicted by our MHD computation with that of the source-surface model (e.g. Schatten et al. 1969; Altschuler and Newkirk 1969; Hoeksema 1991; Wang & Sheeley 1988; Wang & Sheeley 1992), a frequently used

3

tool for approximating heliospheric structure. Ulysses' latitude position for this time period (near 30° S latitude) is also shown. The source-surface model predicts crossings for this time period, whereas the MHD simulation correctly predicts no HCS crossings.

During February–April of 1995 (before and after the spacecraft approached perihelion) the Ulysses spacecraft sampled a wide range of heliographic latitude in a short period of time. Figure 3 shows the HCS predicted by our MHD computation for CR1892, the start of this fast latitude scan. Also shown is the Ulysses trajectory projected in solar latitude and Carrington longitude (back at the Sun) and published Ulysses HCS crossings indicated by crosses (Smith et al. 1995). The different line colors on the trajectory plots indicate the Carrington rotation at that time. During CR1892 (the time period for which the calculation is most valid), the two Ulysses crossings occur almost exactly where predicted by the MHD computation. Later in time (CR1893 and CR1894), the overall shape of the MHD HCS agrees well with Smith et al.'s empirically derived HCS, but the Ulysses crossings occur above the HCS. The reason for this can be seen in Figure 3, which shows the predicted source-surface model for the 3 rotations. The source-surface model suggests that the solar magnetic field is changing during this time period, as evidenced by the changing HCS. Therefore, MHD computations of CR1893 and CR1894 are required for a complete comparison; this work is presently underway. We are also investigating how solutions obtained with magnetograms from the National Solar Observatory at Kitt Peak during this time period compare with those obtained from Wilcox data.

While the favorable comparisons between our computational results and coronal and heliospheric observations are encouraging, it should be noted that there are also some differences between our simulations and observations. Fine-scale details of the corona do not appear in our computations. Higher resolution magnetograms (such as those from Kitt Peak or the SOI/MDI instrument aboard SOHO), coupled with higher resolution computations, may help to capture some of these fine-scale features. Streamers in eclipse images typically show a stronger nonradial tendency than in our the computations. This may be related to the poor estimation of polar fields in the Wilcox data, due to projection effects, and may also be improved by
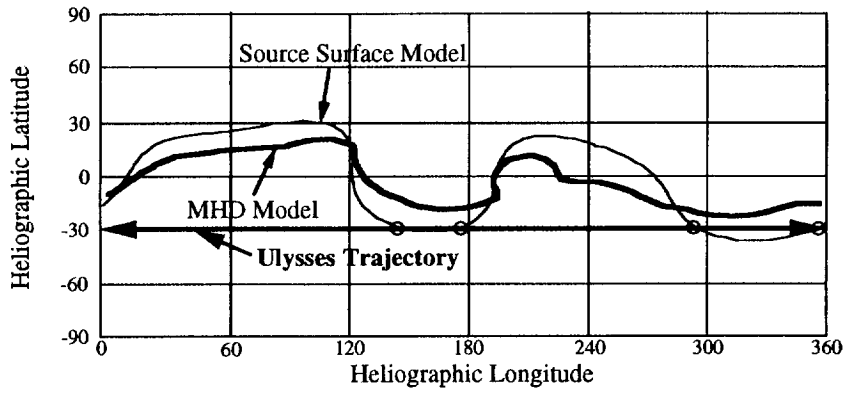
4

Figure 2. A comparison of the heliospheric current sheet predicted by the source-surface model and an MHD calculation for Carrington rotation 1869 (May10 - June 6, 1993). The Ulysses spacecraft, which did not observe current sheet crossings during this rotation, was situated at 30°S latitude. The red circles indicate the crossings predicted by the source-surface model.
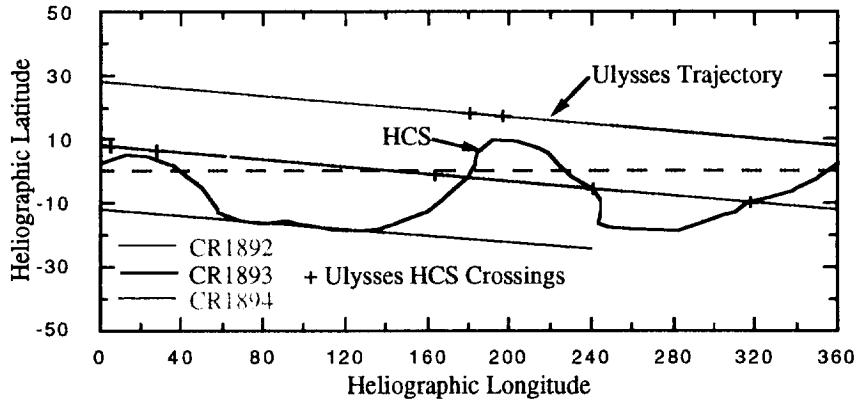

Figure 3. The heliospheric current sheet (HCS) predicted by the MHD model for Carrington rotation 1892, with the Ulysses trajectory for the fast-latitude scan superimposed. HCS crossings identified by Smith et al. (1995) are indicated by black crosses. The times of the different rotations (CR1892, CR1893, and CR1894) are color-coded on the trajectory plot.
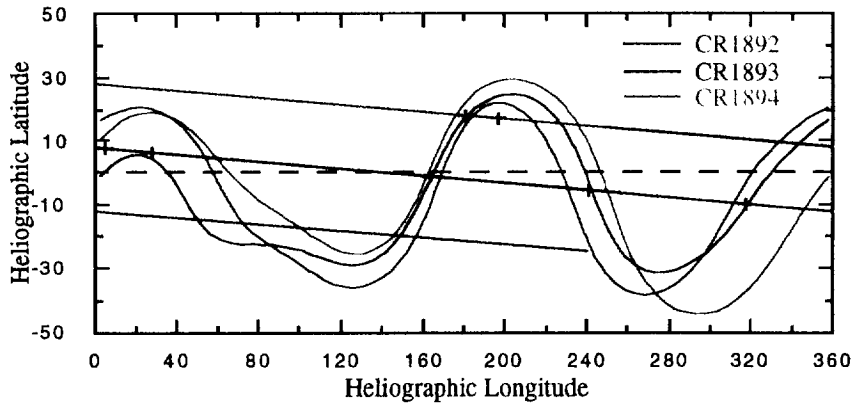

Figure 4. Variation of the heliospheric current sheet predicted by the source-surface model for the rotations occuring during the fast-latitude scan. The extent of the HCS varies during this time period.

5

better magnetograms. Most important, our computations (using a polytropic energy equation) fail to reproduce the fast (800 km/s) solar wind observed by Ulysses at high latitude. Improvement of this aspect of the calculation requires an energy equation that treats the complicated thermodynamic processes occurring the solar corona and solar wind more realistically. In the past year we have begun to investigate solar wind solutions where the effects of coronal heating, thermal conduction parallel to the magnetic field, and the acceleration of the solar wind by Alfvén waves are included. In these solutions the lower boundary is in the transition region, rather than the base of the corona, so energy loss by radiation must also be considered. Our preliminary 1D and 2D calculations including these effects show promising results (Mikić et al. 1996ab), and further investigation of these solutions is ongoing.

(c) A Model of the Corona and Inner Heliosphere at Solar Minimum

Sophisticated investigation of coronal mass ejections (CMEs) requires using a realistic model of the background corona for the initial condition. Guided by our experience with the Wilcox photospheric magnetic field data and our comparisons with eclipse images, we developed a model configuration of the solar corona (and its extension to 1 A.U.) at solar minimum. We specified an initial magnetic flux distribution of the form:

$$B_r = A_0 cos^3\theta + A_1 sin^2\theta cos2\phi + A_2 sin^3\theta sin3\phi \tag{7}$$

with $A_0 = 13.3$ Gauss, $A_1 = 1.3$ Gauss, $A_2 = 0.33$ Gauss, and the distribution rotated by -20° around the y axis. We then computed an equilibrium configuration by integrating the MHD equations to steady state, with the additional constraint that the Sun's rigid rotation rate was imposed (corresponding to a sidereal period of 26 days). The resulting configuration is shown in Figure 5. The magnetic field lines and polarization brightness near the Sun (Fig. 5a and 5b) show a configuration similar to that often seen at solar minimum. As we move farther from the Sun, the magnetic field lines show the expected spiral behavior (Figure 5d shows the field lines out to 1 astronomical unit; 1 A.U. $= 1.49 \times 10^6$ km $= 214$ solar radii).

Using this configuration as a starting point, we have begun to investigate how
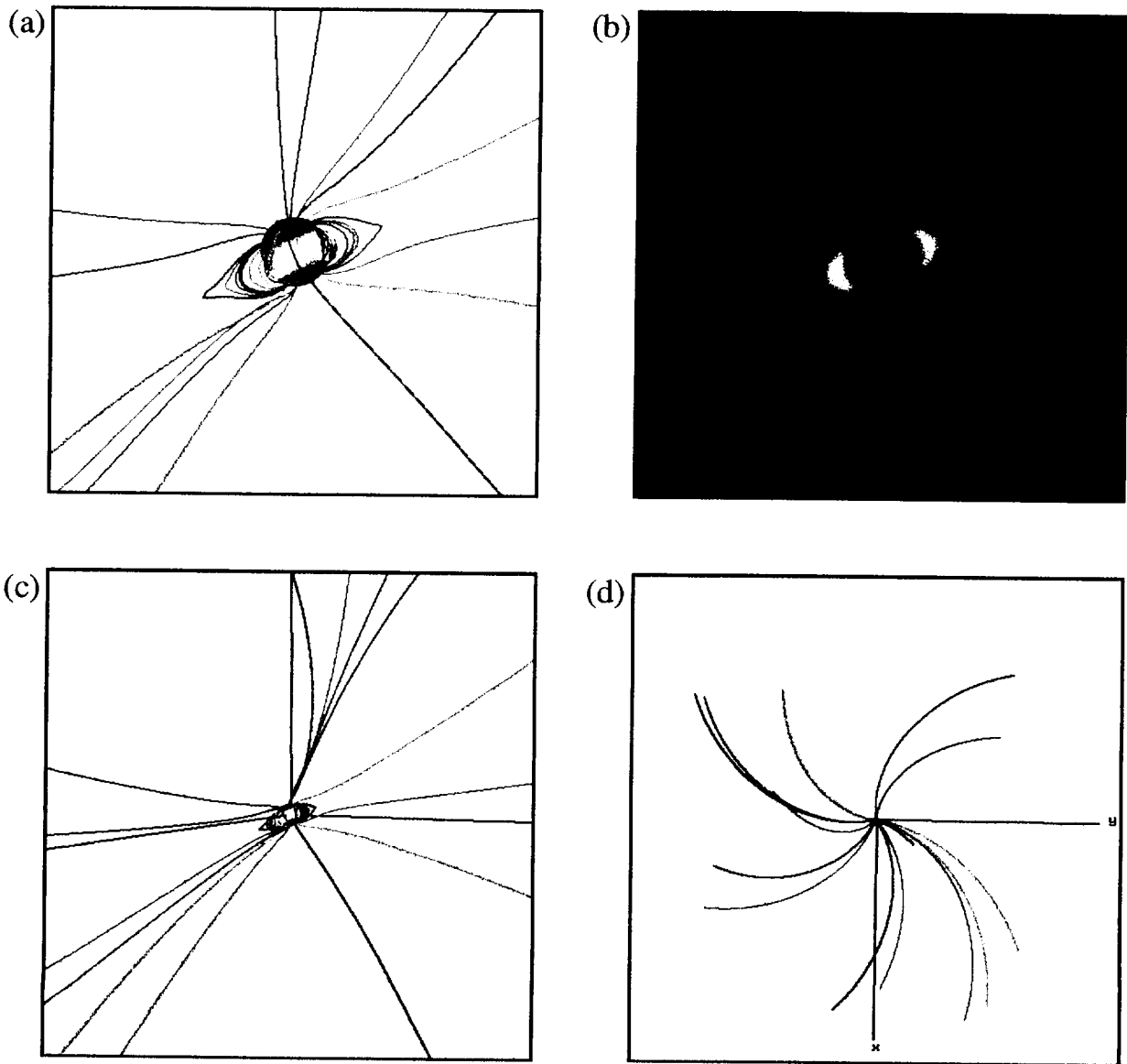
6

Figure 5. An MHD simulation of the solar corona and inner heliosphere for a solar-minimum type configuration. The computation is performed in the inertial frame, so the magnetic flux distribution on the Sun rotates rigidly. (a) Field lines viewed close to the Sun, showing a helmet streamer configuration. (b) polarization brightness from the same view as (a). (c) Field lines from the same view angle as (a) and (b), but farther from the Sun. (d) Field lines viewed from 1 A.U. above the Sun's North pole. The spiral structure is apparent. Field lines that appear "shorter" actually are receding from or approaching the viewpoint.

CMEs can be initiated in the corona, as well as studying the effects of CME propagation through the corona and heliosphere. These results are described by Linker and Mikić (1997) and Mikić and Linker (1997).

(d) Future Work

In the coming year we expect to continue research in all of the areas we have described progress in for the last year. To improve our coronal and heliospheric modeling, we plan to perform similar calculations to those described here using Kitt Peak and SOHO/MDI magnetograms. These higher resolution magnetograms may allow us to capture features not resolvable from Wilcox data, and may allow a better determination of the polar fields, which can strongly influence the solution. We also plan to continue our development of solutions with more realistic thermodynamics, and to perform comparisons of these solutions with interplanetary data. With this approach we hope to be able to understand the coronal sources of the fast and slow solar wind. Finally, we plan further investigations of how coronal structures can be disrupted and coronal mass ejections initiated, as well as the heliospheric consequences of these events.

(e) Publications

Linker, J. A., Z. Mikić & D. D. Schnack, Global coronal modeling and space weather prediction, in *Solar Drivers of Interplanetary and Terrestrial Disturbances*, (K. S. Balasubramaniam, S. L. Keil, & R. N. Smartt, eds.), Astron. Soc. Pac. Conf., *95*, 208, 1996.

Linker, J. A., & Z. Mikić, Extending Coronal Models to Earth Orbit, in *Coronal Mass Ejections: Causes and Consequences*, submitted, 1997.

Mikić, Z., & J. A. Linker, Large scale structure of the solar corona and inner heliosphere, *Solar Wind 8*, AIP Conf. Proceedings 382, 104, 1996.

Mikić, Z., & J. A. Linker, The initiation of coronal mass ejections by magnetic shear, in *Coronal Mass Ejections: Causes and Consequences*, submitted, 1997.

This contract also partially or fully supported 5 invited and 6 contributed presentations at scientific meetings in the past year.

References

Altschuler, M. D., & G. Newkirk, *Sol. Phys.*, *9*, 131, 1969.

Hoeksema, J. T., Tech. Rep. CSSA-ASTRO-91-01, Center for Space Science and Astronomy, Stanford University, California, 1991.

Linker, J. A., Z. Mikić & D. D. Schnack, in *Solar Drivers of Interplanetary and Terrestrial Disturbances*, (K. S. Balasubramaniam, S. L. Keil, & R. N. Smartt, eds.), Astron. Soc. Pac. Conf., *95*, 208, 1996.

Linker, J. A., & Z. Mikić, in *Coronal Mass Ejections: Causes and Consequences*, submitted, 1997.

Mikić, Z., & J. A. Linker, *Solar Wind 8*, AIP Conf. Proceedings 382, 104, 1996.

Mikić, Z., & J. A. Linker, in *Coronal Mass Ejections: Causes and Consequences*, submitted, 1997.

Mikić, Z., J. A. Linker & J. A. Colborn, *EOS Trans. AGU*, *77*, (Spring AGU Meeting) 1996a.

Mikić, Z., J. A. Linker & J. A. Colborn, AAS/SPD Meeting, Madison, Wisconsin, 1996b.

Parker, E. N., *Interplanetary Dynamical Processes*, Interscience publishers, New York, 1963.

Schatten, K. H., J. M. Wilcox & N. Ness, *Solar Phys.*, *6*, 442, 1969.

Smith, E. J., M. Neugebauer, A. Balogh, S. J. Bame, G. Erdos, R. J. Forsyth, B. E. Goldstein, J. L.Phillips & B. Tsurutani, *Geophys. Res. Lett.*, *20*, 2327, 1993.

Smith, E. J., A. Balogh, M. E. Burton, G. Erdos & R. J. Forsyth, *Geophys. Res. Lett.*, *22*, 3325, 1995.

Wang, Y. M. & N. R. Sheeley, *J. Geophys. Res.*, *93*, 11, 227, 1988.

Wang, Y. M. & N. R. Sheeley, Jr., *Astrophys. J.*, *392*, 310, 1992.